Quantum phase transitions in the Rabi-Stark model at finite frequency ratios

Xiang-You Chen¹, You-Fei Xie¹, and Qing-Hu Chen^{1,2,*}

¹ Department of Physics and Zhejiang Province Key Laboratory of Quantum

Technology and Device, Zhejiang University, Hangzhou 310027, China

² Collaborative Innovation Center of Advanced Microstructures, Nanjing University, Nanjing 210093, China

(Dated: December 21, 2024)

In this work, we observe a continuous quantum phase transition in the Rabi-Stark model at finite ratios of the qubit and cavity frequencies if the nonlinear stark coupling strength is twice of the cavity frequency, in contrast to the quantum Rabi model where the quantum phase transition only emerges in the infinite frequency ratio. The quantum criticality of the Rabi-Stark model is then analyzed in terms of the energy gap, the order parameter, as well as the fidelity. The critical exponents are derived analytically. The finite size scaling analysis for the order parameter and the fidelity susceptibility is also performed. Several finite size exponents are then extracted from the universal scaling. The size independent energy gap exponent suggests the Rabi-Stark model and the quantum Rabi model are not in the same universality class, while the correlation length exponent could be the same with the specified definition of the effective system size.

PACS numbers: 03.65.Yz, 03.65.Ud, 71.27.+a, 71.38.k

I. INTRODUCTION

As advocated by Anderson that more is different [1], emergent phenomena occur when systems with many particles behave differently than their original few ones. In classical systems the transition between different phases is driven by thermal fluctuations. Similarly, quantum fluctuations can lead to transitions between distinct quantum phases of matter, such as superconductors and insulators [2]. Recently, the quantum Rabi model (QRM) [3] and Javnes-Cummings model [4], both only describe a single-mode cavity field and a two-level atom, but interestingly exhibit the continuous quantum phase transition (QPT) [5–7], seem extending the previous concept to systems with few degrees of freedom. To see the collective behaviors, one need enhance the atom-field interaction and increase the two level energy difference at the same time. The former requirement can be gradually satisfied with the recent progress on cavity quantum electrodynamics (QED) [9], circuit QED [10–12], and trapped ions [13], which can realize the QRM from strong coupling [14], ultra-strong coupling [15], and even to deep-strong coupling [16].

The light-matter interaction can be engineered in many different ways. Benefiting from development of quantum simulation technology, the so-called quantum Rabi-Stark model (RSM) has been realized by adding an nonlinear process to the QRM [17, 18], and the Hamiltonian is given by

$$H_R = \left(\frac{\Delta}{2} + \frac{U}{2}a^{\dagger}a\right)\sigma_z + \omega a^{\dagger}a + g(a^{\dagger} + a)\sigma_x, \quad (1)$$

where Δ and ω are frequencies of two-level system and cavity, $\sigma_i(i=x,y,z)$ are usual Pauli matrices describing the two-level system, a (a^{\dagger}) are the annihilation (creation) bosonic operators of the cavity mode with frequency ω , and g denotes the linear coupling strength between the qubit and the cavity. The nonlinear cou-

pling strength U is determined by the dispersive energy shift. It has been studied by the Bargmann approach [19, 20] and the more physical Bogoliubov operator approach [21]. It is found that the emergent Starklike nonlinear interaction bring about the novel and exotic physical properties. Such as, the interaction induced energy spectra collapse can be observed in the limit of $U/\omega \to \pm 2$ [21] above a critical atom-cavity coupling strength. Here the first-order QPT, indicated by the level crossing of the ground-state and first excited state, is also observed [21]. Grimsmo and Parkins conjectured that the nonlinear dispersive-type coupling would possibly induce a new superradiant phase at this single atom level if $U/\omega < -2$ [17] in the open systems.

In this work, we find that the equilibrium continuous QPT can also be present in the RSM in the limit of $U/\omega \to \pm 2$ at finite Δ/ω , in sharp contrast to the prerequisite $\Delta/\omega \to \infty$ in the QRM. The paper is structured as follows: In Sec. II, we proposed the evidence of the QPTs in the RSM at finite ratio Δ/ω by studying the singularity of ground state energy based on analytical solutions at $U = \pm 2\omega$. In Sec. III, we focus on critical behavior of ground state energy and exited energy near critical point, and consistently obtain the critical gap exponent both analytically and numerically. We will focus on the critical behavior of order parameter and its finite size scaling behavior in sec. IV. In sec. V, we propose the accurate hypothesis of fidelity susceptibility, and the nice scaling behavior is also observed. Finally we give a summary and outlooks in Sec. VI.

II. QUANTUM CRITICAL POINT

As found by Xie et al. [21], the RSM at U=2 can be mapped to an effective quantum harmonic oscillator. Thus the low energy spectra of Hamiltonian (1) (in units of $\omega=1$) can be given by

$$\frac{\sqrt{-\left(\frac{\Delta}{2} + E\right)\left(E + 1 - \frac{\Delta}{2}\right)}}{\sqrt{-\left(\frac{\Delta}{2} + E + 2g^2\right)}} = 2n + 1, \quad n = 0, 1, 2, \dots \infty.$$
(2)

where an infinite number of discrete energy levels is confined in the energy interval

$$\frac{\Delta}{2} - 1 < E < E_c^+,\tag{3}$$

if $g < g_c^+$, where $g_c^+ = \sqrt{(1-\Delta)/2}$ and $E_c^+ = -\Delta/2 - 2g^2$. All discrete low energy levels collapse to E_c^+ at $g = g_c^+$, thus the energy gap closes at g_c^+ , indicating a QPT in this model. For the case of U = -2, the extension can be achieved straightforwardly by changing

For $g > g_c^+$, it is observed that all energies by numerical exact diagonalization become closer to E_c^+ monotonously with increasing truncated Fock space, although the convergence is hardly achieved by numerics. We argue that the energy would be only E_c^+ $-\Delta/2-2g^2$, and resulting effective harmonic potential, $\omega_{eff} = \sqrt{1 + 2g^2/\left(\frac{\Delta}{2} + E\right)}$, is flat. Thus the spectrum is continuous, and the energy could be any value for the flat potential. But the perquisite condition for flat potential is no other than $E = E_c^+$. It should be stressed that Eq. (2) derived from a quantum oscillator cannot be used to give any real energy for $g > g_c^+$.

The analytical mean photonic number $\overline{n} = \langle a^{\dagger} a \rangle$ in the ground-state is also found to diverge at g_c^+ [21]. Infinite photons are activated at the critical coupling, signifying the emergence of a new quantum phase.

In the next section, we will study critical behavior of the RSM in the effective thermodynamic limit and perform the finite size scaling analysis with a definition of the effective system size.

ENERGY GAP CLOSING AND EXPONENT

First, we analyze the critical exponent for energy gap between the ground-state and the first excited state. Generally, it should also follow the universal scaling behavior in the continuous QPT [2]

$$\varepsilon(g \to g_c) \sim |g - g_c|^{z\nu_x},$$
 (4)

where $z(\nu_x)$ is the (dynamics) critical exponent.

To determine $z\nu_x$ analytically, we rewrite Eq. (2) as

$$\frac{\sqrt{2g^2 + y}(b - y)}{\sqrt{y}} = 2n + 1,\tag{5}$$

where $y = E_c^+ - E$ and $b = 2 (g_c^+)^2 - 2g^2$. Note that both y and b tend to zero when g tends to g_c^+ , which implying that the solution for y must be of the

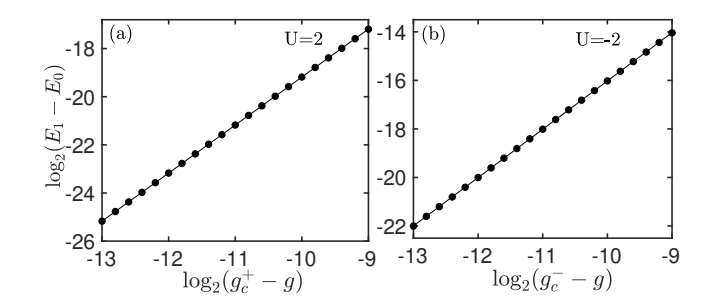


FIG. 1: (Color online) The log-log plot of energy gap $E_1 - E_0$ as a function of $g_c^{\pm} - g$ before g_c at U = 2 (a) and U = -2(b). $\Delta = 0.5$. The slops of both fitting line are about 2.

following form

$$y = rb^2 + O(b^3). (6)$$

By Eq. (5) we can obtain all eigenenergies in the limit $g \to g_c$ as

$$E_n = E_c^+ - \frac{8g^2}{(2n+1)^2} \left[(g_c^+)^2 - g^2 \right]^2,$$
 (7)

implying that energy gap between all nearest energy levels is $E_{n+1} - E_n \propto (g_c^+ - g)^2$. So we can easily obtain the gap exponent for the first two eigenstates as $z\nu_x=2$. This energy gap exponent can be further confirmed with the full solution in Eq. (2) numerically in Fig. 1 where we plot the energy gap $E_1 - E_0$ as a function of $g_c^+ - g$ on a log-log scale. In the critical regime, $g \to g_c^+$, it is obvious that the slop fits the value $z\nu_x=2$. This good agreement is independent of the value of Δ (not shown here).

Meanwhile, the variance of position quadrature of the field is found to diverge as $\Delta x = \frac{1}{2} \langle (a^{\dagger} + a)^2 \rangle \propto (g_c^+ - a)^2 \rangle$ $(g)^{-1}$, as has been given analytically in Eq. (A11) of the Appendix A. It follows that $z = 2, \nu_x = 1$ in the RSM. In both the Dicke model [22] and the QRM [5], the same gap exponent $z\nu_x = 1/2$ with $z = 2, \nu_x = 1/4$ has been found. So the RSM is not in the same equilibrium universality class of the Dicke model and QRM for the different length exponents ν_x .

The phase transition takes places in the thermodynamic limit with the emergence of singularity of some physical observables. Despite few degrees of freedom in the QRM context, the effective system size could be also defined [5] in order to catch sight of the critical behavior of the phase transitions. In the QRM, the effective size is defined as $L = \Delta/\omega$ [5], and the singularity only appears in the limit of $\Delta/\omega \to \infty$.

Since the energy gap closes only at $U = \pm 2$ in the present RSM, we may define the system size here as

$$L = \frac{1}{2 \mp U}. (8)$$

With this definition, $U = \pm 2$ is just corresponding to the thermodynamic limit. We then calculate the groundstate energy and its derivatives at the critical points

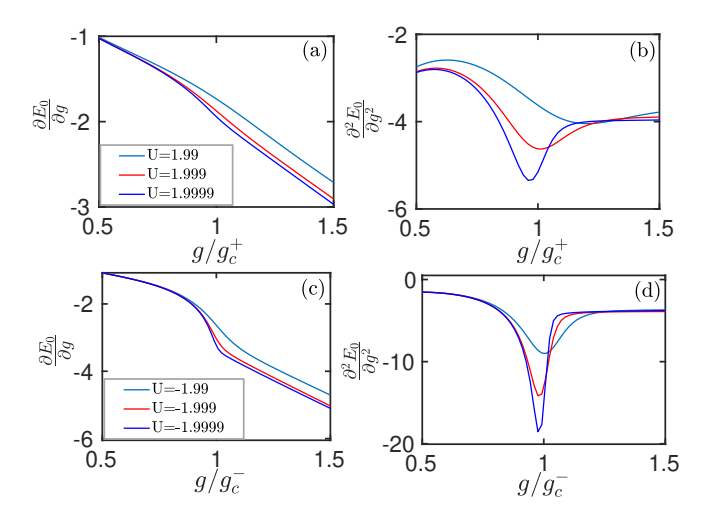


FIG. 2: (Color online) The first- and second-order derivative of the ground-state energy by the numerically exact solution of the RSM at $\Delta=0.5$ for different U approaching to 2 (upper panel) and -2 (lower panel).

 $g_c^\pm = \sqrt{(1\mp\Delta)/2}$ for finite effective sizes L(U), and see how it evolves with the increase of the system size. The exact solution can be obtained by either the G-function approach [21] or the direct exact diagonalizations in truncated Fock space. Figure 2 presents the first-order (left panel) and the second-order (right panel) derivatives of the ground state energy for U gradually approaching to ± 2 , i.e. the size L tends to infinity. One can find that the first-order derivative is always continuous when $U\to\pm 2$, while its second-order derivative changes drastically with system size L, displaying the discontinuity in the trend. It also provides the evidence of the second-order QPT in this model. It should be pointed out that it is extremely difficult to obtain the converged results in the both approaches if U further approaches to ± 2 .

IV. ORDER PARAMETER AND FINITE SIZE SCALING

To characterize the continuous QPT, we should define the order parameter. In QRM [5], the re-scaled cavity photon number $\overline{n} = \langle a^\dagger a \rangle$ can be the order parameter since it is zero below and finite above the critical points. But in this RSM it is always finite below and diverges at the critical point. We may define the inverse photon number $1/\overline{n}$ as the order parameter M. It is finite below g_c , and tends to zero at g_c . In terms of Eq. (7), Eq.(34) in Ref. [21] in the limit of $g \to g_c^+$ may be rewritten as

$$\overline{n} = \frac{6g^2 \left(g_c^{+2} - g^2\right)}{E_c^+ - E_0} + \frac{3}{16\left(g_c^{+2} - g^2\right)} \propto \left(g_c^+ - g\right)^{-1}, (9)$$

Thus the order parameter exponent is $\beta=1$. The detailed derivation of Eq. (9) is also given in Eq. (A10) in the Appendix A.

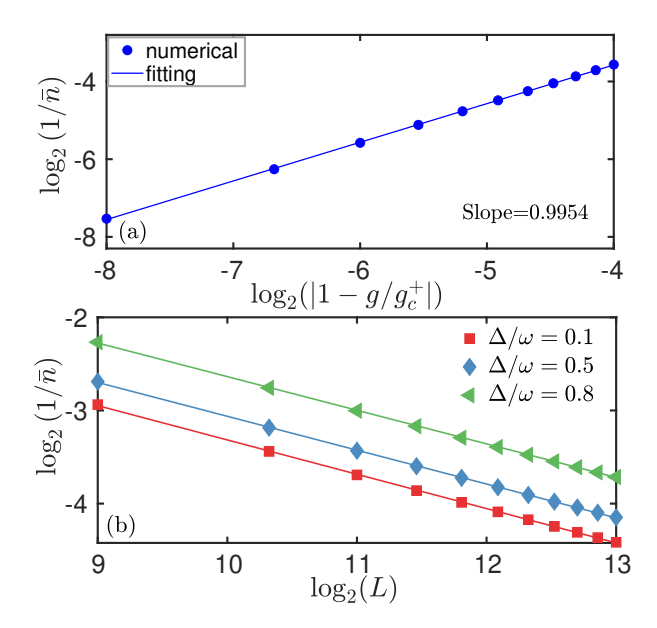


FIG. 3: (Color online) (a) The log-log plot of the order parameter $1/\overline{n}$ as a function of $\left|1-g/g_c^+\right|$ before g_c for U=2 and $\Delta=0.5$, the fitting slope is very close to 1. (b) The log-log plot of order parameter $1/\overline{n}$ as a function of system size L at g_c for U=2 and $\Delta=0.1,0.5,0.8$. All fitting slopes are very close to -1/3.

Figure 3 (a) shows the order parameter $1/\overline{n}$ as a function of the reduced coupling constant $t=1-g/g_c^+$ on a log-log scale before g_c^+ by the numerically exact solution of the RSM.. A very nice power law behavior, $1/\overline{n} \propto |1-g/g_c^+|^\beta$, is clearly shown in the critical regime. The slop of the fitting line indicates that the critical exponent of the order parameter is $\beta=1\pm0.0046$, confirming the analytical findings.

A log-log plot for the order parameter versus different size at the critical point g_c^+ is presented Fig. 3 (b). A perfect power-law behavior, $1/\overline{n} \propto L^{-\gamma}$, is clearly shown. The slops of the fitting lines for all values of Δ give the same scaling exponent $\gamma=1/3$

The finite size scaling for the order parameter can be also performed. In the critical regime of the continuous phase transition, it should satisfy finite scaling ansatz for the homogeneous function $M(\lambda^{h_1}t,\lambda^{h_2}L)=\lambda M(t,L)$

$$M = |t|^{\beta} m(|t|L^{\gamma/\beta}), \tag{10}$$

where β is the order parameter exponent and γ is the finite size scaling exponent for the order parameter. The function m should be universal for large system size in the second-order QPT. $\nu = \gamma/\beta$ is correlation length exponent due to the scaling function Eq. (10).

By the numerically exact solution of the RSM, we show the finite size scaling according to Eq. (10) for different values of L above and below the critical point at U=2 in Fig. 4. Within the two exponents $\beta=1$ and $\gamma=1/3$ obtained above independently, an excellent collapse to the single curve in the critical regime is achieved for different

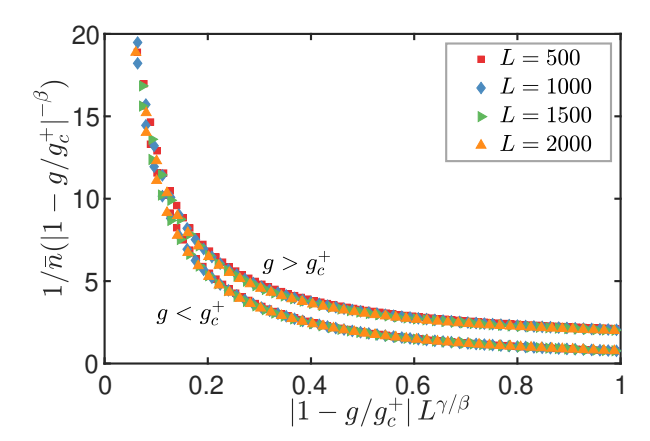


FIG. 4: (Color online) Finite size scaling for order parameter $1/\overline{n}$ according to Eq. (10) for both above and below the critical point at U=2 and $\Delta=0.5$.

large size. Two universal functions above and below the critical points are not required to be the same [5]. The universal scaling behavior observed here corroborates the continuous QPTs in the RSM at U=2.

V. FIDELITY SUSCEPTIBILITY AND FINITE SIZE SCALING ANALYSIS

The ground state fidelity can be taken as an useful tool to detect the QPTs even without the knowledge of the order parameters [23, 24]. It is defined as the overlap of the ground state wavefunctions at very close coupling parameters q and $q + \delta q$ as

$$F(g, \delta g) = |\langle \psi_0(g) | \psi_0(g + \delta g) \rangle|.$$

The singularity of critical point would inevitably leads to the wavefunction experiencing dramatically change when crossing the critical point, showing a sharp change of fidelity.

Correspondingly, the fidelity susceptibility can be defined as [23]

$$\chi_F(g) = \lim_{\delta g \to 0} \frac{-2 \ln F(g, \delta g)}{\delta g^2},$$

and can be written in terms of the eigenstates of the Hamiltonian

$$\chi_F(g) = \sum_{n \neq 0} \frac{|\langle \psi_n(g) | H_I | \psi_0(g) \rangle|^2}{[E_n(g) - E_0(g)]^2},$$
 (11)

which is the leading order of the change in the fidelity.

In the critical regime, the fidelity susceptibility decays in a power law away from the critical point with critical exponent α [24, 25]

$$\chi_F \propto |g - g_c^{\pm}|^{-\alpha}. \tag{12}$$

In terms of the original definition of fidelity susceptibility [26]

$$\chi_F = \left\langle \frac{\partial \Psi_0}{\partial \lambda} \middle| \frac{\partial \Psi_0}{\partial \lambda} \right\rangle - \left\langle \frac{\partial \Psi_0}{\partial \lambda} \middle| \Psi_0 \right\rangle \left\langle \Psi_0 \middle| \frac{\partial \Psi_0}{\partial \lambda} \right\rangle, \quad (13)$$

we can actually derive the critical exponent of fidelity susceptibility $\alpha = 2$ analytically, which is described in the end of the Appendix A.

We present the fidelity susceptibility as a function of the deviation $g_c - g$ on a log-log scale below g_c for $U = \pm 2$ in Fig. 5. All data can be well fitted by straight lines with the same slop -2, so we can immediately obtain its critical exponent $\alpha = 2$, consistent with the analytical derivation.

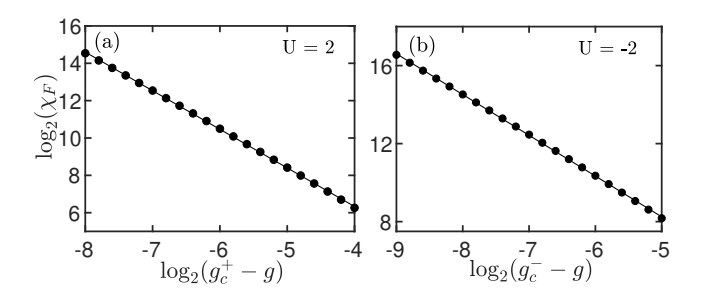


FIG. 5: (Color online) The log-log plot of fidelity susceptibility as a function of $g_c^{\pm} - g$ at $\Delta = 0.5$.

In the second QPTs, the average fidelity susceptibility should follow the following finite-scaling ansatz [23, 27]

$$\frac{\chi_F^{max} - \chi_F(g)}{\chi_F(g)} = f[(g - g_m)L^{\nu}], \tag{14}$$

where g_m is the coupling strength of the maximum fidelity susceptibility, f is the scaling function, and ν is the correlation length critical exponent.

This function should be universal for large L in the second-order QPTs. As shown in Fig. 6, with $\nu=1/3$, an excellent collapse in the critical regime is achieved according to Eq. (14) in the curves for large effective sizes L. Beyond the critical regime, the collapse becomes poor. As L increases, the curves tend to converge in the wider coupling regime. It is demonstrated that ν is an universal constant. Interestingly, the correlation length exponent obtained here is the same as that obtained from the finite size scaling ansatz in the order parameter in the last section. The average FS diverges as the system size increases at the critical point, demonstrating a Landau-type transitions in the Rabi-Stark model.

The insets of Fig. 6 show fidelity susceptibility at the maximum point as a function of the system size L for both $U=\pm 2$ on a log-log scale. A nice power law behavior $\chi_F^{max} \propto L^{\mu}$ is shown at large L. The finite size exponents extracted from all curves tend to a converging value $\mu=2/3$.

In terms of the finite size scaling ansatz in Eq. (14), the critical exponents should satisfy the scaling law as $\mu/\nu=\alpha$, where α is just the fidelity susceptibility critical exponent. Obviously, $\alpha=2$ here is the same as the independent calculation given in Fig. 5, as well as the analytical derivation in the Appendix A.

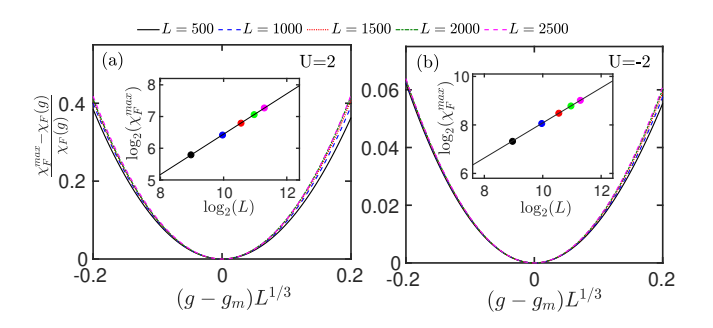


FIG. 6: (Color online) The finite size scaling for the fidelity susceptibility according to Eq. (14) for different system size L for U=2 (a) and U=-2 (b). $\Delta=0.5$. The corresponding size L dependence of the maximum fidelity susceptibility χ_F^{max} is presented in the insets.

The finite size scaling analysis for the fidelity susceptibility has been performed for the Dicke model [27], and the correlation length exponent is obtained to be $\nu=2/3$, which is the same as that in Lipkin-Meshkov-Glick model [25]. Recently, the similar study was done on the QRM using the effective size $L=\Delta/\omega$, and the same correlation length exponent was obtained [28]. Until now, no any different critical behavior of the continuous QPT has been observed in the Dicke model, Lipkin-Meshkov-Glick model, as well as the QRM in the infinite frequencies ratio.

However, the critical exponents μ and ν obtained from the finite size scaling analysis in the RSM here are different from those in the Dicke model [27] and the QRM [28]. Note that these two exponents are size L dependent. If we redefine the system size as $L' = \sqrt{L}$ in Eq. (8), then the scaling exponents μ and ν for the fidelity are the same as Dicke model and the QRM. The fidelity critical exponent α is actually independent of the size, and also can be determined by the ratio of two size dependent exponent μ/ν . Interestingly, it is just the same as in the Dicke model and the QRM.

VI. SUMMARY

In conclusion, we have discovered the QPT in the RSM at $U=\pm 2$ from the energy gap closing, the universal critical behavior of the order parameter and the fidelity. The critical exponents for several observables can be analytically obtained: The energy gap exponent is $z\nu_x=2$ with $z=2,\nu_x=1$, the critical exponent of the inverse photon number, which can regard as the order parameter of RSM, is $\beta=1$, and the critical exponent of fidelity susceptibility is $\alpha=2$. All these critical exponents have also been confirmed by the numerical exact solutions to the RSM.

By using the effective system size $L=1/(2\mp U)$ for $U\to\pm 2$, the finite size scaling analysis for both the order parameter and the fidelity susceptibility has been performed. The size scaling exponent of the order parameter is found to be $\gamma=1/3$. Two size exponents of the fidelity susceptibility are also obtained by the perfect finite size scaling, which ratio recover the size independent critical exponent of the fidelity susceptibility $\alpha=2$. All these consistent picture provide a strong evidence of the second-order QPT in this model.

We have found that the energy gap exponent in the RSM is different from that in the QRM [5] due to different critical exponents of $\nu_x^{RSM}=1$ and $\nu_x^{QRM}=1/4$ despite the same dynamic exponent z=2. While the critical exponents of the fidelity susceptibility $\alpha=2$ are identical in both models. The two size independent critical exponents for the energy gap and the fidelity susceptibility, respectively, show different behavior, suggesting that these two models would belong to different universality classes, but be related inherently.

Below the critical points, we find the ground-state has a conserved parity symmetry, odd parity for U=2, and even parity for U=-2. Above the critical points, the parity symmetry is broken due to the infinite degeneracy for all states. We then speculate gapless Goldstone mode excitations above the critical points in this model.

We like to point out that the QPT found in the RSM is of practical importance in two aspects. One is that we do not need the extreme condition for the occurrence of the QPT like the infinite ratio of the qubit and frequency Δ/ω in the QRM. In the present RSM, the frequency ratio Δ/ω allowed for phase transitions can be any values. The other one is that for U positively twice of the cavity frequency, the critical coupling is $g_c^+ = \sqrt{(1-\Delta)/2},$ which can be weak in the resonance regime, and can be as weak as one like by tuning the qubit frequency. This QPT should be experimentally feasible in any cavity-atom coupling device, such as the cavity (circuit) QEDs and the ion-trap. The price paid is to incorporate the nonlinear Stark coupling between the two-level system and the fields in the devices.

ACKNOWLEDGEMENTS This work is supported by the National Science Foundation of China (Nos. 11674285, 11834005), the National Key Research and Development Program of China (No. 2017YFA0303002).

* Corresponding author. Email:qhchen@zju.edu.cn.

Appendix A: Analytical derivation of some critical exponents of the RSM at U=2

In this Appendix, we derive some critical exponent analytically based on the analytical exact solutions to the RSM at U=2. We will first briefly review the previous solution in the framework of the Fock space [29], then we present the exact eigenfunction.

In terms of the basis of σ_z , the Hamiltonian (1) in the

matrix form can be written as

$$H_0 = \begin{pmatrix} 2a^{\dagger}a + \frac{\Delta}{2} & g\left(a^{\dagger} + a\right) \\ g\left(a^{\dagger} + a\right) & -\frac{\Delta}{2} \end{pmatrix}. \tag{A1}$$

The series expansion of the eigenfunction in the Fock space is

$$|\Psi\rangle = \begin{pmatrix} |\Psi_1\rangle \\ |\Psi_2\rangle \end{pmatrix} = \begin{pmatrix} \sum_n^\infty e_n |n\rangle \\ \sum_n^\infty f_n |n\rangle \end{pmatrix}. \tag{A2}$$

where e_n and f_n are the expansion coefficients, $|n\rangle$ is the number states. The Schrödinger equation then gives

$$\left(2a^{\dagger}a + \frac{\Delta}{2}\right) \sum_{n=0}^{\infty} e_n |n\rangle + g\left(a^{\dagger} + a\right) \sum_{n=0}^{\infty} f_n |n\rangle = E \sum_{n=0}^{\infty} e_n |n\rangle,$$
(A3)

$$g\left(a^{\dagger}+a\right)\sum_{n=0}^{\infty}e_{n}\left|n\right\rangle = \left(\frac{\Delta}{2}+E\right)\sum_{n=0}^{\infty}f_{n}\left|n\right\rangle.$$
 (A4)

By inspection of Eq. (A4), we obtain

$$\sum_{n=1}^{\infty} f_n |n\rangle = \frac{g(a^{\dagger} + a)}{\frac{\Delta}{2} + E} \sum_{n=1}^{\infty} e_n |n\rangle,$$

Inserting it into Eq. (A3) leads to the effective Hamiltonian for the bosonic wavefunction in the upper level $|\Psi_1\rangle$

$$H_{eff} = 2a^{\dagger}a + \chi(a^{\dagger} + a)^2 + \frac{\Delta}{2},$$
 (A5)

with $\chi = \frac{g^2}{\frac{\Delta}{2} + E}$.

To diagonalize the Hamiltonian above, we apply the squeezing transformation $S = \exp\left[\frac{r}{2}(a^2 - a^{\dagger^2})\right]$ with $r = \frac{1}{4}\ln(\frac{1}{1+2\chi})$, and then get a Hamiltonian for a quantum oscillator

$$H' = SH_{eff}S^{\dagger} = \sqrt{1 + 2\chi}(2a^{\dagger}a + 1) - 1 + \frac{\Delta}{2}.$$
 (A6)

The eigenenergy E is obviously given by

$$E = \sqrt{1 + 2\chi}(2n + 1) - 1 + \frac{\Delta}{2}, \quad n = 0, 1, 2...\infty.$$
 (A7)

which further results in Eq. (2).

The eigenfunction to the harmonic oscillator is

$$|n\rangle_s = S^{\dagger} |n\rangle = e^{-\frac{r}{2}(a^2 - a^{\dagger 2})} |n\rangle$$
 (A8)

Thus the eigenfunction for the RSM at U=2 for the low spectra reads

$$|\Psi_n\rangle = \frac{1}{N_n} \begin{pmatrix} c_n S^{\dagger} | n \rangle \\ d_n S^{\dagger} (a^{\dagger} + a) | n \rangle \end{pmatrix}$$
 (A9)

where $c_n = (1+2\chi_n)^{-1/4}$ and $d_n = \chi_n/g$, and the normalization factor $N_n = \sqrt{c_n^2 + (2n+1)d_n^2}$. Several quantities can be calculated using this eigenfunction. For convenience, we denote the dimensionless coupling parameter $\lambda = g/g_c^+$.

First, we calculate the mean photon number using the wave function of Eq. (A9) as

$$\langle a^{\dagger} a \rangle = \frac{1}{N_n^2} [c_n^2 \langle n | S a^{\dagger} a S^{\dagger}] | n \rangle$$

$$+ d_n^2 \langle n | (a^{\dagger} + a) S a^{\dagger} a S^{\dagger} (a^{\dagger} + a) | n \rangle]$$

$$= \frac{1}{N_n^2} \{ c_n^2 (n \cosh 2r + \sinh^2 r)$$

$$+ d_n^2 [(2n^2 + n + 1) \cosh 2r + (2n + 1) \sinh^2 r + n(n + 1) \sinh 2r] \}$$

$$\simeq \frac{3}{8} \frac{(2n + 1)^2 + 1}{(1 - \Delta)(1 - \lambda^2)} \propto (1 - \lambda)^{-1}. \tag{A10}$$

where the limit $g \to g_c$ is performed in the last step. This is just Eq. (9) for the order parameter in the main text.

Then we turn to the variance of position quadrature of the field Δx . By using $x = 1/\sqrt{2}(a^{\dagger} + a)$, we have

$$\Delta x = \langle x^2 \rangle - \langle x \rangle^2 = \frac{1}{2} \langle (a^{\dagger} + a)^2 \rangle$$

$$= \frac{e^{2r}}{2N_n^2} \left[c_n^2 (2n+1) + d_n^2 (6n^2 + 6n + 3) \right]$$

$$\simeq \frac{3 \left[(2n+1)^2 + 1 \right]}{4(1-\Delta) (1-\lambda^2)} \propto (1-\lambda)^{-1}. \tag{A11}$$

The critical exponent $\nu_x = 1$ for the position fluctuation is obtained, which is part of the gap exponent in the main text.

Finally we calculate the ground state fidelity susceptibility χ_F in the limit of $g \to g_c^+$, by using its the differential form (13). The eigenfunction of n-th energy level in this limit can be written as

$$|\Psi_n\rangle = \begin{pmatrix} C_n S^{\dagger}(|n\rangle) \\ D_n S^{\dagger}(a^{\dagger} + a) |n\rangle \end{pmatrix},$$
 (A12)

where

$$C_n \simeq \frac{(1-\Delta)\lambda}{2n+1} \sqrt{2(1-\lambda^2)},$$

 $D_n \simeq \sqrt{\frac{1}{2n+1}}.$

Now, we can calculate the first-order partial derivative of the ground state wave function with respect to λ

$$\left| \frac{\partial \Psi_0}{\partial \lambda} \right\rangle = \begin{pmatrix} \left(\frac{\partial C_0}{\partial \lambda} \right) S^\dagger + C_0 \left(\frac{\partial S^\dagger}{\partial \lambda} \right) |n\rangle \\ D_0 \left(\frac{\partial S^\dagger}{\partial \lambda} \right) \left(a^\dagger + a \right) |n\rangle \end{pmatrix},$$

where

$$\frac{\partial S^{\dagger}}{\partial \lambda} = -\frac{1}{2} \frac{\partial r(\lambda)}{\partial \lambda} S^{\dagger} (a^2 - a^{\dagger^2}) \tag{A13}$$

$$\frac{\partial r}{\partial \lambda} = -\frac{1}{2(1+2\gamma)} \frac{\partial \chi}{\partial \lambda} \simeq \frac{\lambda}{1-\lambda^2}.$$
 (A14)

Some overlaps in Eq. (13) are list below after lengthy calculation

$$\left\langle \frac{\partial \Psi_0}{\partial \lambda} \middle| \frac{\partial \Psi_0}{\partial \lambda} \right\rangle \simeq \frac{(1 - \Delta)^2 (2 + \lambda^4)}{(1 - \lambda^2)} + \frac{3\lambda^2}{2 (1 - \lambda^2)^2},$$
(A15)

$$\left\langle \Psi_0 \middle| \frac{\partial \Psi_0}{\partial \lambda} \right\rangle \simeq -2(1-\Delta)^2 \lambda + \frac{3\lambda}{(1-\lambda^2)}, \text{ (A16)}$$

$$\left\langle \frac{\partial \Psi_0}{\partial \lambda} \middle| \Psi_0 \right\rangle \simeq -2(1-\Delta)^2 \lambda - \frac{3\lambda}{(1-\lambda^2)}. \text{ (A17)}$$

Finally, we arrive at the fidelity susceptibility in the limit to the critical point

$$\chi_F \simeq \frac{(1-\Delta)^2 (2+\lambda^4)}{(1-\lambda^2)} + \frac{21}{2} \frac{\lambda^2}{(1-\lambda^2)^2}$$

$$\propto (1-\lambda)^{-2}, \tag{A18}$$

which explicitly yields the critical exponent for the fidelity susceptibility as $\alpha = 2$.

- P. W. Anderson. More Is Different. Science, 177, 393 (1972).
- [2] S. Sachdev, *Quantum Phase Transitions*, 2nd ed. (Cambridge University Press, Cambridge, England, 2011).
- [3] I. I. Rabi, Phys. Rev. **51**, 652 (1937).
- [4] E. T. Jaynes and F. W. Cummings Proc. IEEE 51, 89(1963).
- [5] M.-J. Hwang, R. Puebla, and M. B. Plenio, Phys. Rev. Lett.115, 180404 (2015);
- [6] M.-J. Hwang and M. B. Plenio, Phys. Rev. Lett. 117,123602 (2016).
- [7] M. X. Liu, S. Chesi, Z. J. Ying, X. S. Chen, H. G. Luo, and H. Q. Lin, Phys. Rev. Lett. 119, 220601 (2017).
- [8] D. Braak, Q. H. Chen, M. Batchelor, and E. Solano, J. Phys.A: Math. Gen. 49, 300301 (2016).
- [9] J. M. Raimond, M. Brune, and S. Haroche, Rev. Mod. Phys. 73, 565 (2001).
- [10] T. Niemczyk et al., Nature Physics 6, 772 (2010).
- [11] F. Yoshihara, T. Fuse, S. Ashhab, K. Kakuyanagi, S. Saito, and K. Semba, Nat. Phys. 13, 44 (2016).
- [12] P. Forn-Díaz, J. J. García-Ripoll, B. Peropadre, J. L. Orgiazzi, M. A. Yurtalan, R. Belyansky, C. M. Wilson, and A. Lupascu, Nat. Phys. 13, 39 (2016).
- [13] D. Leibfried, R. Blatt, C. Monroe, and D. Wineland, Rev. Mod. Phys. 75, 281 (2003).
- [14] J. Clarke and F. K. Wilhelm, Nature 453, 1031 (2008).
- [15] P. Forn-Díaz et al., Phys. Rev. Lett. 105, 237001 (2010).

- [16] J. Casanova, G. Romero, I. Lizuain, J. J. García-Ripoll and E. Solano, Phys. Rev. Lett. 105 263603 (2010).
- [17] A. L. Grimsmo and S. Parkins, Phys. Rev. A 87 033814 (2013).
- [18] A. L. Grimsmo and S. Parkins, Phys. Rev. A 89 033802 (2014).
- [19] A. J. Maciejewski, M. Przybylska, and T. Stachowiak, Phys. Lett. A 379 1503(2015).
- [20] H. P. Eckle and H. Johannesson, J. Phys. A: Math. Theor. 50, 294004 (2017).
- [21] Y. F. Xie, L. W. Duan, Q. H. Chen, J. Phys. A: Math. Theor. 52, 245304 (2019).
- [22] C. Emary and T. Brandes, Phys. Rev. E 67, 066203(2003); Phys. Rev. Lett. 90, 044101(2003).
- [23] W. L. You, Y. W. Li, and S. J. Gu, Phys. Rev. E 76, 022101 (2007).
- [24] S. J. Gu, H. M. Kwok, W. Q. Ning and H. Q. Lin, Phys. Rev. B, 77,245109(2008).
- [25] H. M. Kwok, W. Q. Ning, S. J. Gu, and H. Q. Lin, Phys. Rev. E 78, 032103(2008).
- [26] S. J. Gu, Int. J. Mod. Phys. B 24, 4371 (2010).
- [27] T. Liu, Y. Y. Zhang, Q. H. Chen and K. L., Wang, Phys. Rev. A 80, 023810(2009).
- [28] B. B. Wei and X. C. Lv, Phys. Rev. A.97, 013845(2018).
- [29] Y. F. Xie and Q. H. Chen, Commun. Theor. Phys. 71 623 (2019).